

Characterizing physiological noise in the brainstem: passband SSFP vs. GRE-EPI

R. H. Tijssen¹, M. Jenkinson¹, P. Jezzard¹, and K. L. Miller¹
¹FMRIB Centre, Oxford University, Oxford, Oxon, United Kingdom

Introduction. Functional MRI of the brainstem is complicated by: 1) small grey matter nuclei, 2) severe distortions due to susceptibility boundaries and 3) high levels of physiological noise, all of which make conventional GRE-EPI BOLD problematic. SSFP fMRI has the potential to produce high-resolution images with reduced distortions [1-3], and recent work reported reduced physiological noise for SSFP in cortical regions [5]. SSFP may therefore be amenable to fMRI of the brainstem and other “hard to image” regions of the brain. However, this previous study [5] had several shortcomings if one is interested in brainstem fMRI: 1) SSFP was compared to a short T_E/T_R variant of GRE (i.e., spoiled gradient echo, or SPGR) rather than GRE-EPI, 2) no inferior regions were covered and 3) no information was provided about the relative contribution of respiratory and cardiac fluctuations. The present work addresses these issues by comparing different physiological noise components in passband SSFP, SPGR (i.e., GRE with acquisition matched to SSFP) and GRE-EPI.

Methods. *Data acquisition.* GRE-EPI, SPGR, and pbSSFP data (Fig.1) were acquired from 7 healthy volunteers on a 3T Siemens scanner (Siemens, Erlangen). The GRE-EPI acquisition is representative of more conventional fMRI acquisitions, while the SPGR data uses the same acquisition to SSFP, enabling one to disentangle effects due to sequence contrast (reflected in SPGR only) and effects due to readout strategy (reflected in GRE-EPI, as well). For each pulse sequence a single coronal slice (matrix=128x128, resolution=2x2x2.5mm) through the brainstem and motor cortex was acquired every 152 ms to temporally resolve physiological fluctuations (2000 volumes, 5 min). GRE-EPI parameters: $\alpha=90^\circ$, $T_R/T_E=152/30$ ms, 1860 Hz/pix. SSFP and SPGR parameters: $\alpha=30^\circ$, $T_R/T_E=9/3.5$ ms, 1860 Hz/pix, 8 lines per T_R . For the SSFP sequence the RF increment was set to place as much of the slice as possible in the SSFP pass band. The SPGR acquisition was identical to SSFP, but included RF and gradient spoiling. Heart and respiration rate were monitored using pneumatic bellows and a pulse oximeter, and scanner triggers were recorded to synchronize the data with the image acquisition.

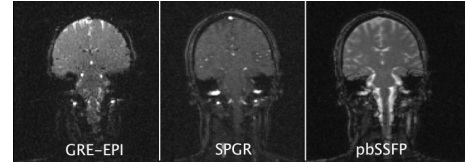


Figure 1: Images as acquired with each sequence illustrating slice location and image quality.

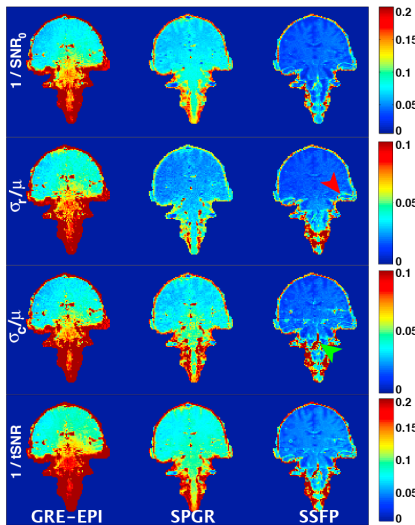


Figure 3: Maps showing the various noise components in a typical subject. From top to bottom: SNR_0^{-1} , normalized cardiac noise, normalized respiratory noise, and $tSNR^{-1}$.

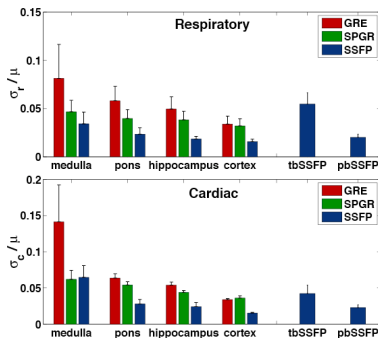


Figure 4: ROI analysis. The normalized respiratory (top) and cardiac noise (bottom) averaged over 7 subjects. Errorbars give inter-subject variability.

References. [1] Scheffler et al. NMR Biomed 2001;14(7):490-496. [2] Miller et al. MRM 2003;50(4):675-683 [3] Bowen et al. ISMRM 2005 p.119 [4] Kruger et al. MRI 2001;46(4): 631- 637 [5] Miller et al. NIMG 2007;37(4):1227-1236 [6] Lee et al. MRM 2006;55(5):1197-1201

Analysis. A linear trend was removed before Fourier transforming each voxel timecourse to generate its power spectra. The integral over the entire power spectrum reflects the total noise present in the data, and consists of a white noise component (the spectral baseline) and additive physiological noise (the peaks at the respiratory and cardiac frequency and their harmonics) (Fig 2). To enable direct comparison of the noise components across the three sequences, we normalize the noise variance by the square of the temporal mean, μ : $\frac{\sigma_{tot}^2}{\mu^2} = \frac{\sigma_0^2 + \sigma_r^2 + \sigma_c^2}{\mu^2}$,

where σ_x (with $x = 0, r, \text{ or } c$) represents the white, respiratory, or cardiac noise, respectively. The individual SNR components can then be calculated by $SNR_x = \mu/\sigma_x$. The respiratory and cardiac frequency bands were determined from physiological recordings by fitting a Gaussian distribution to each frequency spectrum and setting boundaries to 2σ on either side of the centre frequency. Maps showing the fluctuations at cardiac and respiratory frequencies were generated by integrating the relevant peak over this frequency range. In addition to voxel-wise maps, regions of interest including the brainstem (medulla and pons), the hippocampus, and the cortex were analyzed.

Results and Discussion. Figure 2 gives an illustration the power-spectra averaged over the brainstem in a single subject. Enhanced signal fluctuations relative to baseline are observed in the respiratory band (0.3 Hz), the cardiac band (1.3 Hz) and its first harmonic (2.6 Hz). Due to the reduced read-out efficiency (i.e. duty cycle) of GRE-EPI and the spoiling of transverse magnetization in SPGR, these sequences have a lower SNR_0 compared to SSFP, which is reflected by the elevated level of white noise in their power-spectrum (see also Fig 3, top). Maps representing the contribution of the individual noise components are shown in Fig. 3, including the total noise variance ($tSNR^{-1}$) map. All maps demonstrate increased signal variation in the inferior regions of the brain. This is due to the increased B_0 fluctuations caused by respiratory and cardiac pulsation of the cerebral arteries and CSF. Overall, SSFP showed the smallest signal variability in terms of global effects. However, SSFP did show increased sensitivity to respiration in the transition bands of SSFP (red arrow) and in some subjects, pulsatile effects of the basilar artery (green arrow). A group analysis of noise components in the different ROIs is displayed in Fig. 4. For all ROIs, SSFP exhibits smaller noise variance in both the cardiac and respiratory bands compared to GRE-EPI and smaller or statistically similar noise variance compared to SPGR. An additional ROI that was manually drawn around the areas that lie in the transition bands of the SSFP images illustrates that transition band SSFP (tbSSFP) is much more sensitive to physiological noise, in particularly to respiratory effects. This effect results from the strong sensitivity of SSFP to frequency shifts in the transition band, and agrees with previous reported findings [6]. Our results indicate a two-fold increase in temporal SNR for SSFP compared to GRE. However, we have only considered the noise components, without consideration of the BOLD signal change due to actual brain activation. A reasonable predictor of contrast-to-noise ratio (e.g. z-statistic) would be the ratio of signal change to temporal variation (σ_{tot}). A previous study using visual stimulation and acquiring data with comparable sequences and similar echo times reported a 2% signal change for pbSSFP and 5% change for GRE/SPGR [5]. Combining our study with those results, the contrast-to-noise ratio is predicted to be comparable for SSFP and GRE-EPI.

Conclusions. Passband SSFP shows lower signal fluctuations at cardiac and respiratory frequencies compared to conventional GRE-EPI. This may mitigate the expected lower signal changes due to a predominantly T_2 BOLD contrast in pbSSFP. These findings, in conjunction with the ability to obtain high-resolution, low-distortion images, may make pbSSFP an attractive option for brainstem fMRI.

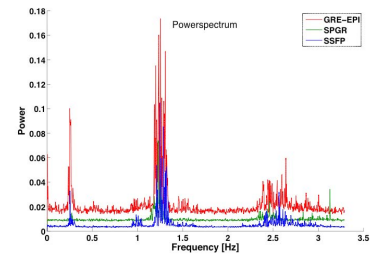


Figure 2: The power spectra of GRE-EPI, SPGR, and SSFP averaged over voxels within the brainstem (single subject).